Applied Physics Letters

Machine-learning-assisted space-transformation accelerates discovery of high thermal conductivity alloys

Cite as: Appl. Phys. Lett. **117**, 202107 (2020); https://doi.org/10.1063/5.0028241
Submitted: 03 September 2020 . Accepted: 08 November 2020 . Published Online: 19 November 2020

Dhvaneel Visaria, and Ankit Jain

View Online Export Citation CrossMark

ARTICLES YOU MAY BE INTERESTED IN

A hybrid self-aligned MIS-MESFET architecture for improved diamond-based transistors
Applied Physics Letters **117**, 202101 (2020); https://doi.org/10.1063/5.0023662

Carrier localization in self-organized quantum dots: An interplay between quantum and solid mechanics
Applied Physics Letters **117**, 202103 (2020); https://doi.org/10.1063/5.0032110

Heterogeneous direct bonding of diamond and semiconductor substrates using NH_3/H_2O_2 cleaning
Applied Physics Letters **117**, 201601 (2020); https://doi.org/10.1063/5.0026348

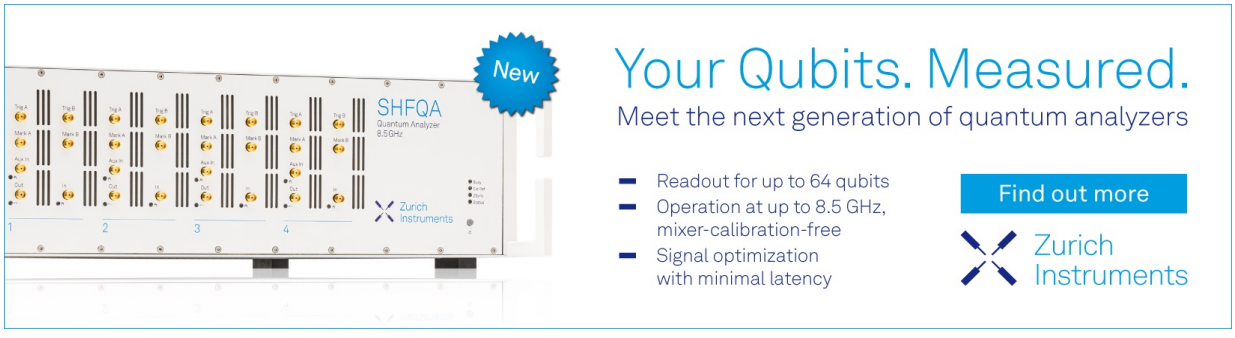

© 2020 Author(s).

Applied Physics Letters ARTICLE scitation.org/journal/apl

Machine-learning-assisted space-transformation accelerates discovery of high thermal conductivity alloys

Cite as: Appl. Phys. Lett. **117**, 202107 (2020); doi: 10.1063/5.0028241
Submitted: 3 September 2020 · Accepted: 8 November 2020 ·
Published Online: 19 November 2020

View Online Export Citation CrossMark

Dhvaneel Visaria and Ankit Jain[a)]

AFFILIATIONS

Mechanical Engineering Department, IIT Bombay, Mumbai 400076, India

[a)]Author to whom correspondence should be addressed: a_jain@iitb.ac.in

ABSTRACT

We study the thermal conductivity distribution of hypothetical graphene-like materials composed of carbon and heavy carbon atoms. These materials are representative of alloys and disordered materials, which are relatively unexplored for thermal properties owing to their large configuration spaces. Since the full thermal conductivity calculations using the Boltzmann transport equation based solutions are computationally prohibitive for each of the 2^{32} considered configurations, we employ regularized autoencoders, a class of generative machine learning models that transform the configuration space to the latent space in which materials are clustered according to the target property. Such conditioning allows selective sampling of high thermal conductivity materials from the latent space. We find that the model is able to learn the underlying thermal transport physics of the system under study and is able to predict superlattice-like configurations with high thermal conductivity despite their higher mass.

Published under license by AIP Publishing. https://doi.org/10.1063/5.0028241

Thermal conductivity is a complex material property involving the interplay of mass density, sound speed, lattice constant, and lattice anharmonicity. The earliest model to predict the thermal conductivity of solids was devised by Slack for crystalline materials.[1] Subsequently, much progress has been made in calculating the thermal transport in crystalline solids, for instance, using the first-principles-based lattice dynamics calculations and molecular dynamics simulations.[2] With the advent of such techniques, numerous material systems have been identified, which exhibit a deviation from the Slack thermal transport model.[3,4] Among other factors, these developments are facilitated by advances in computational resources. However, even with these advances in the computational resources, the thermal transport in alloys and disordered materials is still unexplored owing to the prohibitively massive size of the materials configuration space.

In this regard, machine learning (ML) models are especially useful since they can be easily trained to learn the thermal transport behavior from the known/training dataset, and these trained models can be further used to predict the thermal transport properties of new material configurations involving the participation of the same atomic species. Such a simple application of ML models has already been used to predict the variety of material properties varying from ionic conductance,[5] crystal thermal conductivity,[6] thermoelectric figure of merit,[7] and optoelectronic properties[8,9] to mechanical strength,[10] nuclear fuel systems,[11] and drug discovery.[12] Most of these ML applications in materials science are mainly focused on either fitting a surrogate on-the-go machine learning model for exploring pre-defined finite-sized material search space or training the ML model to predict desired properties for a new given material. However, for alloys and disordered solids, the search space is exponentially large. Simply using a surrogate on-the-go or pre-trained ML model in such cases would require an exponentially large number of ML model evaluations, which is not viable with the existing computational resources.

A relatively new class of ML models, called generative models, are useful in the exploration of these exponentially large material search spaces. These trained models provide a mapping from a given search space to the latent space in which the materials with desired properties are clustered together [Fig. 1(b)]. Therefore, sampling using interpolation or other related techniques can be employed to design new materials with desired properties. Such models have been used in materials research recently to discover new compounds from vanadium–oxygen phase-space for battery applications[13] and to generate images of hypothetical materials with tailored optical properties using the absorption spectrum data of a wide range of material quinary and quaternary oxides.[14]

Published under license by AIP Publishing

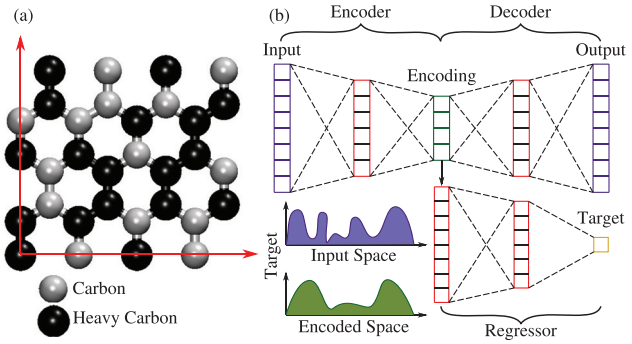

FIG. 1. (a) 32-atom unit cell of the model graphene-like two-dimensional materials and (b) schematic depicting feature-space transformation using an autoencoder in conjunction with a regressor. The clustering is achieved by setting the target to the desired material property in (b).

Here, we demonstrate the use of such ML models for searching materials with desired thermal properties by considering hypothetical graphene-like two-dimensional materials as a test system. In particular, we search for high thermal conductivity materials from the search space of 2^{32} model graphene-like structures generated by placing a carbon atom or a heavy carbon atom (twice as heavy as carbon, i.e., 24 a.m.u.) at the lattice sites of the 32-atom graphene unit cell (constructed by 4×2 replications of the 2-atom primitive unit cell) [see Fig. 1(a)]. We use an autoencoder-based ML model consisting of a convolutional neural-network-based encoder/decoder in conjunction with a feedforward neural-network-based thermal conductivity regressor. We find that this ML model attains a root mean square error (RMSE) of 7 W/m K on predicted thermal conductivity, indicating considerably high conformance of the model predictions with the computationally expensive Boltzmann Transport Equation (BTE) based solution. Furthermore, we find that the ML model is able to learn the right underlying thermal transport physics from the training data, and it predicted high thermal conductivity for superlattice like configurations even though no such configurations were used in the training dataset.

We calculate the thermal conductivities of the model graphene structures by solving the BTE under the relaxation time approximation along with the Fourier law as[15,16]

$$k_x = \sum_i c_{ph,i} v_{x,i}^2 \tau_i. \quad (1)$$

The summation in Eq. (1) is over all the phonon modes in the Brillouin zone, and c_{ph}, $\mathbf{v}$, and τ are the phonon specific heat, group velocity, and scattering lifetime, respectively. The phonon specific heat is obtained using the Bose–Einstein statistics as $c_{ph,i} = \frac{\hbar\omega_i}{V}\frac{\partial n_i^o}{\partial T} = \frac{k_B x_i^2 e^{x_i}}{(e^{x_i}-1)^2}$, where $x_i = \hbar\omega_i/k_B T$, and $\hbar$, ω_i, V, n_i^o, T, and k_B are the reduced Planck constant, phonon frequency, crystal volume, Bose–Einstein distribution $[n_i^o = 1/(e^{x_i} - 1)]$, temperature, and Boltzmann constant. The phonon group velocities are obtained from the derivative of phonon frequencies with respect to phonon wavevectors, $\mathbf{q}$, as $v_{x,i} = \partial\omega_i/\partial q_x$. The phonon frequencies and scattering rates are obtained from the diagonalization of the dynamical matrix and three-phonon scattering processes, respectively. Further details regarding the phonon dynamical matrix and scattering rate calculations are detailed in Refs. 16 and 17.

The interatomic interactions between carbon atoms are described using the optimized Tersoff model fitted to graphite and diamond.[18] All thermal conductivity calculations are performed at a temperature of 300 K using a 32 atom unit cell as in Fig. 1(a). Using these settings, the thermal conductivity is obtained for the material having all carbon atoms in its unit cell configuration, i.e., the thermal conductivity of graphene is 717 W/m K, which is in perfect agreement with the literature reported values.[19] The hypothetical materials are created by varying the mass of one or more of the 32 carbon atoms in the unit cell, i.e., by replacing carbon atoms with heavy carbon atoms. Note that the interatomic interactions are kept fixed, and only atomic masses are varied for the generation of new materials.

The dependence of thermal conductivity on atomic masses is presented in Fig. 2(a). In the dataset, the thermal conductivity (k_x) is larger than 600 W/m K only for configurations consisting of either all carbon atoms or all heavy carbon atoms. The thermal conductivity decreases rapidly with the introduction of a heavy carbon (carbon) atom in all carbon (heavy carbon) atom configurations. This sudden decrease is due to the strong Rayleigh-like scattering of phonons from mass-disorder/defects and has been reported for Si/Ge[20] and PbTe/PbSe[21] alloys. However, unlike the high-disorder-limit treatment of phonon scattering using Tamura's theory in these literature studies

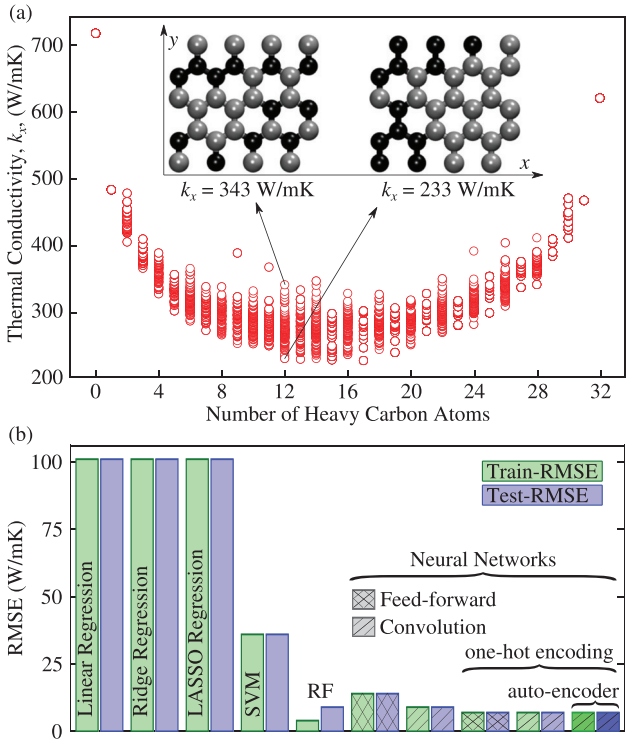

FIG. 2. (a) The thermal conductivity k_x, dataset obtained by varying the number of heavy carbon atoms in the 32-atom graphene unit cell of Figs. 1(a) and 1(b), and the performance of different ML models on the k_x-dataset. The variation of k_x for a given number of heavy atoms is due to their relative spatial arrangement [inset in (a)].

Published under license by AIP Publishing

(thus providing only the lower-bound on the thermal conductivity[22]), the disorder is explicitly handled using the phonon-phonon scattering in this study. This explicit accounting of disorder results in variations in thermal conductivity even for a fixed number of heavy carbon atoms in the unitcell due to local ordering of light/heavy atoms [see the inset of Fig. 2(a)].

The simplest model to predict the mass dependence of lattice thermal conductivity is devised by Slack, according to which the thermal conductivity of simple semiconductors decreases monotonically with the average atomic mass, $\bar{m}$, of the participating atoms as $1/\bar{m}$.[1] This model fails drastically in compound semiconductors (semiconductors with more than one atomic species, as in the present case) due to the acoustic-optical phonon bandgap and acoustic phonon bunching as has been reported earlier.[3,4] Furthermore, for materials with high Debye temperature (such as graphene with a Debye temperature of 1800 K), the quantum phonon occupation effects are significant and are not accounted for by the Slack model, thus resulting in further deviations from the $1/\bar{m}$ scaling.

Although the mass dependence of the thermal conductivity values can be explicitly calculated using the BTE-based solution, these calculations are computationally expensive and require, for instance, around 10 cpu-hours per material on modern cpus. Therefore, we switch to ML models to accelerate the discovery of these graphene-like materials with high thermal conductivity values from the exponentially large search space. For this, we explicitly calculate the thermal conductivities for 1800 unique configurations as reported in Fig. 2(a). For ML training, we artificially engineer the k_x-dataset to ensure equal contributions (150 instances) from all mass ratios (defining the mass-ratio as the ratio of the number of heavy carbon atoms to the total number of atoms in the unit cell). This is done so that the model does not develop a bias toward a particular mass-ratio, consequently affecting thermal conductivity prediction since k_x is dependent on mass of the atoms [as can be seen from Fig. 2(a)].

Furthermore, since calculated thermal conductivities correspond to periodic repetitions of the unit cell extending infinitely in the two-dimensional space, we invoke the translational invariance to augment the training dataset. We identify 16 translational symmetries, thereby resulting in a total of 79 200 data points in the augmented dataset. Finally, we divide this k_x-dataset in the ratio of 7:3 for training and testing of the ML models. In the case of neural-network-based ML models, we also transform the unit cell representation (feature-vector) from the one-dimensional 32-bit mass vector to a two-dimensional 8×4 mass matrix [corresponding to Fig. 1(a)] to take advantage of this image-like representation of the unit cell.

We start by first testing the performance of the conventional ML models as implemented in the Python library Scikit-learn.[23] As mentioned earlier, these models are inadequate for such exponentially large search spaces; nevertheless, these models are easy to interpret and provide guidance for design/training of more complex, neural network based models. The results obtained from these conventional models are summarized in Fig. 2(b).

With linear regression, using a simple 32-bit mass vector as the input feature vector, the obtained root mean square error (RMSE) is 100 and 101 W/m K for training and testing datasets. This large value of RMSE is expected as the thermal conductivity of crystalline materials varies non-linearly with atomic masses (especially, at low temperatures where quantum effects are more pronounced, as is the case for graphene-like hypothetical materials considered here at 300 K) as presented in Fig. 2(a). As is evident from similar train and test RMSEs, there is no over-fitting in the linear model, and therefore, no improvement in performance is observed with the introduction of $L2$ and $L1$ regularizations with Ridge[24] ($\alpha = 70$) and least absolute shrinkage and selection operator (LASSO)[25] ($\alpha = 0.023$) regression, respectively.

With the introduction of non-linearity in the form of radial basis function kernel and kernel coefficient (γ) equal to "scale" (as defined in the scikit-learn library) in the support-vector machine,[26] the train/test RMSE reduces to 36 W/m K. Further reduction in training error is observed with a random forest regressor with 100 trees (and by preserving other default settings). However, it is inferred that this is a case of over-fitting since the test RMSE is more than twice as much as the train RMSE.

We next switch to neural network based regressors to leverage their ability to learn and model non-linear and complex relationships. We test both feed-forward and convolutional neural networks along with binary and one-hot encoding for carbon and heavy carbon atoms. We find that even with binary encoding for atomic masses, the performances of feed-forward and convolution networks are superior to those of the support-vector machine. The binary encoding, however, misleads the networks by suggesting that subtraction of a light atom from another heavy atom results in a light atom. To avoid this misrepresentation, we adopt one-hot encoding and test the performances with both feed-forward and convolution neural networks. The resulting train and test RMSEs are only 7 W/m K for both the networks. These results are comparable to the performance of the random forest model but without any over-fitting.

To take advantage of exceptionally low RMSE values realized using neural-network-based regressors, we next implement autoencoders in conjunction with such regressors so as to enable direct sampling of unit cell configurations with desired properties. An autoencoder consists of an encoder and a decoder. They are designed to replicate the input at the output. The encoder compresses the input to a lower-dimensional latent space in the bottleneck layer, while the decoder reconstructs the output from the latent space. The compression captures the more important information from the input data while filtering out the extraneous information. Here, we employ convolutional neural networks for the encoder and the decoder and a feed-forward network for regression along with the one-hot encoding as is reported in Fig. 3(a).

The 32-bit feature array representing the unit cell configuration in the dataset is reshaped into an $8 \times 4 \times 2$ array using the one-hot encoding (i.e., a light carbon atom is denoted by [0, 1], while a heavy carbon atom is denoted by [1, 0]). The thermal conductivity values of all the configurations in the dataset are normalized using its mean and standard deviation to ensure stable convergence of weights and biases in the neural network. We employ a sequence of two convolutional layers in the encoder, which eventually flattens out to the latent space of dimension 32. Each of the convolutional layers uses a (4×4) kernel with a random normal initializer and a (1×1) stride. The filter sizes are 16 and eight for the first and second convolutional layers, respectively. The padding is such that the height and the width of the array remain unchanged. The hyperbolic tangent (tanh) activation is used at the output of each of the nodes barring the input to the latent space. The decoder is built by replicating the encoder architecture in reverse. The feed-forward regressor, consisting of one hidden layer with tanh

Published under license by AIP Publishing

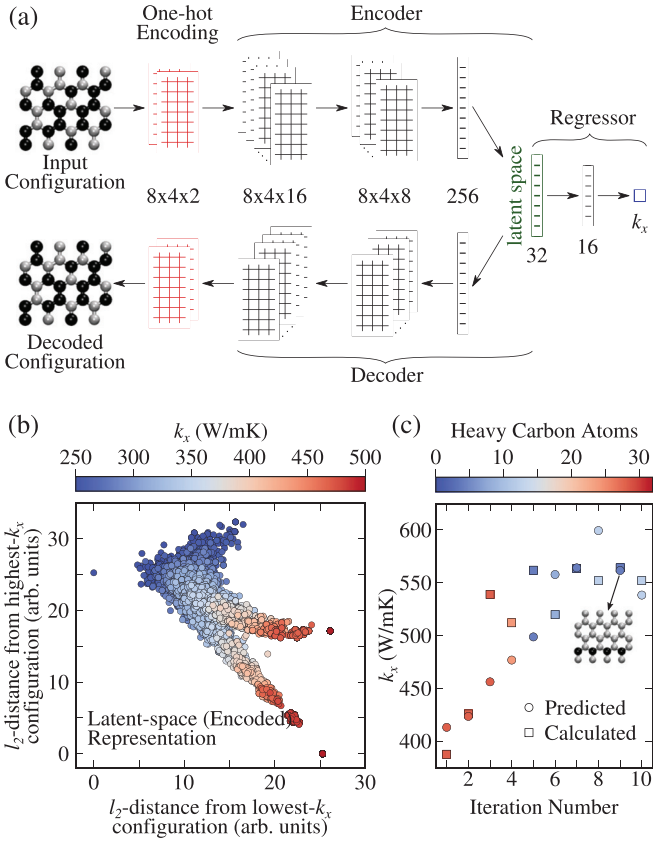

FIG. 3. (a) Architecture of the convolutional autoencoder in conjunction with the feed-forward regressor, (b) clustering of data points in the latent space of the autoencoder according to their corresponding thermal conductivity value, k_x, and (c) highest k_x sample predictions and the corresponding calculated values using interpolation sampling followed by BTE-based calculations for 10 iterations.

activation, predicts the thermal conductivity value. The training is performed to minimize the mean-squared error loss at the decoder and the feed-forward regressor outputs using the "Adam" optimizer for 500 epochs and batch-size equal to 1024, and equal weights are assigned to the autoencoder reconstruction and the regressor losses.

Using this autoencoder, the RMSE obtained from the regressor on the test dataset is 7 W/m K, which is the same as that obtained from the convolution network. Furthermore, the reconstruction error obtained from the decoder is 7.07×10^{-3}, i.e., amongst 4.4 reconstructed configurations of the 32-atom unit cell, only one bit of any one of the configuration is wrongly reproduced, thus indicating regeneration of original configurations from the latent space.

Since the presence of the thermal conductivity regressor regularizes the training of the autoencoder, the configurations in the trained latent space of the encoder are clustered together on the basis of the material thermal conductivity, k_x [as can be seen in Fig. 3(b)]. We leverage this spatial conditioning of the unit cell configurations in the latent space to sample new configurations with desired thermal conductivity values. We utilize the interpolation approach for sampling new materials by choosing points that are a linear combination of any two known latent space points in the high thermal conductivity cluster. The high-k_x sampled data points are transformed to the original unit cell configuration space using the decoder, and the thermal conductivity of these configurations is predicted by feeding their latent space representation to the regressor.

We perform this sampling iteratively to find high-k_x configurations from intermediate mass ratios in the range of 0.125–0.875. We start by sampling unit-cell configurations of new hypothetical materials having the mass ratios in this given range. We next choose 30 sampled materials with the highest predicted k_x and calculate their true k_x values using explicit BTE based calculations. Next, the model as in Fig. 3(a) is trained on the augmented dataset including the new sampled materials, and then, a new set of high-k_x materials are sampled. The process is repeated until no further improvement is observed in the highest-k_x of sampled unit cell configurations.

We find that this iterative procedure converges after 10 iterations to a hypothetical material with the predicted and calculated k_x of 564 W/m K. [Fig. 3(c)]. As shown in the inset of Fig. 3(c), this high-k_x material corresponds to a unit cell configuration with superlattice like stacking of atomic ribbons with a mass ratio of 0.125. This predicted k_x is 44.6% higher than the highest k_x in the training dataset in Fig. 2(a) for the same mass ratio. It is interesting to note that (i) the thermal conductivity value of the sampled highest k_x material (having four heavy atoms in its unit cell) is 16.5% larger than that of the unit cell configuration with only one heavy atom and (ii) the ML model is able to identify this high-k_x superlattice-like configuration although no such configuration is present in the initial training dataset [Fig. 2(a)].

Since we attain a very high k_x value for this superlattice-like unit cell configuration, we hypothesize that such an ordered stacking of light and/or heavy atomic ribbons could lead to exceptional thermal transport. We calculate the thermal conductivity values of the unit cell configurations with an equal number of light and heavy atomic ribbons (4 each) stacked alternately in groups of 1, 2, and 4 using the BTE-based solution. Interestingly, we obtain exceptionally high k_x values for the alternately stacked unit configuration of mass ratio 0.5 (i.e., alternate rows of the heavy and light carbon atoms in the unit cell configuration) of 597 W/m K, which even surpasses the sampled highest k_x material. Although this higher k_x material shows that the ML-guided search does not guarantee a global extremum, it demonstrates that the ML model is able to capture the right thermal transport physics, which could be used in conjunction with human understanding to accelerate the search of novel materials with desired material properties. Since phonon relaxation time due to disorder scattering determines the thermal conductivity of alloys, a similar methodology could be adopted in future work by setting the relaxation time as the target property.

In summary, using hypothetical graphene-like disordered two-dimensional materials as the test case, we demonstrate the applicability of the generative machine learning models to explore massively large search spaces of alloys/disordered materials for desired thermal properties. In comparison to conventional ML models, which require an exponentially large number of model evaluations to scan such search spaces, the generative ML models expedite materials discovery by mapping materials to a latent space where they are clustered according to the target property. This mapped latent space can be sampled to discover materials with desired target properties. Hence, this ML-guided framework accelerates the material search many-fold and provides invaluable insights to steer the exploration toward an optimum solution.

Published under license by AIP Publishing

DATA AVAILABILITY

The data that support the findings of this study are available from the corresponding author upon reasonable request.

REFERENCES

[1]G. Slack, J. Phys. Chem. Solids **34**, 321 (1973).
[2]L. Lindsay, C. Hua, X. Ruan, and S. Lee, Mater. Today Phys. **7**, 106 (2018).
[3]L. Lindsay, D. A. Broido, and T. L. Reinecke, Phys. Rev. Lett. **111**, 025901 (2013).
[4]A. Jain and A. J. H. McGaughey, J. Appl. Phys. **116**, 073503 (2014).
[5]A. D. Sendek, E. D. Cubuk, E. R. Antoniuk, G. Cheon, Y. Cui, and E. J. Reed, arXiv:1808.02470 (2018).
[6]H. Wei, S. Zhao, Q. Rong, and H. Bao, Int. J. Heat Mass Transfer **127**, 908 (2018).
[7]T. Wang, C. Zhang, H. Snoussi, and G. Zhang, Adv. Funct. Mater. **30**, 1906041 (2020).
[8]A. L. Moore and L. Shi, Mater. Today **17**, 163 (2014).
[9]E. Pop, Nano Res. **3**, 147 (2010).
[10]L. Lu, M. Dao, P. Kumar, U. Ramamurty, G. E. Karniadakis, and S. Suresh, Proc. Natl. Acad. Sci. **117**, 7052 (2020).
[11]E. J. Kautz, A. R. Hagen, J. M. Johns, and D. E. Burkes, Comput. Mater. Sci. **161**, 107 (2019).
[12]C. Réda, E. Kaufmann, and A. Delahaye-Duriez, Comput. Struct. Biotechnol. J. **18**, 241 (2020).
[13]F. Noé, S. Olsson, J. Köhler, and H. Wu, Science **365**, eaaw1147 (2019).
[14]H. S. Stein, D. Guevarra, P. F. Newhouse, E. Soedarmadji, and J. M. Gregoire, Chem. Sci. **10**, 47 (2019).
[15]J. M. Ziman, *Electrons and Phonons* (Oxford University Press, Clarendon, Oxford, 1960).
[16]J. A. Reissland, *The Physics of Phonons* (John Wiley and Sons Ltd., 1973).
[17]A. J. McGaughey, A. Jain, H.-Y. Kim, and B. Fu, J. Appl. Phys. **125**, 011101 (2019).
[18]L. Lindsay and D. A. Broido, Phys. Rev. B **81**, 205441 (2010).
[19]L. Lindsay, D. A. Broido, and N. Mingo, Phys. Rev. B **82**, 115427 (2010).
[20]J. Garg, N. Bonini, B. Kozinsky, and N. Marzari, Phys. Rev. Lett. **106**, 045901 (2011).
[21]Z. Tian, J. Garg, K. Esfarjani, T. Shiga, J. Shiomi, and G. Chen, Phys. Rev. B **85**, 184303 (2012).
[22]S.-I. Tamura, Phys. Rev. B **27**, 858 (1983).
[23]F. Pedregosa, G. Varoquaux, A. Gramfort, V. Michel, B. Thirion, O. Grisel, M. Blondel, P. Prettenhofer, R. Weiss, V. Dubourg, J. Vanderplas, A. Passos, D. Cournapeau, M. Brucher, M. Perrot, and E. Duchesnay, J. Mach. Learn. Res. **12**, 2825 (2011).
[24]A. E. Hoerl and R. W. Kennard, Technometrics **12**, 55 (1970).
[25]R. Tibshirani, J. R. Stat. Soc. **58**, 267 (1996).
[26]C. Cortes and V. Vapnik, Mach. Learn. **20**, 273 (1995).

Published under license by AIP Publishing